ARTICLE

www.the-innovation.org

Primate preoptic neurons drive hypothermia and cold defense

Zhiting Zhang,[1,2,6] Liang Shan,[1,2,6] Yuyin Wang,[1,3,6] Wenfang Li,[1] Minqing Jiang,[1] Feng Liang,[1] Shijing Feng,[1] Zhonghua Lu,[1,2,3,4] Hong Wang,[1,2,3,5,*] and Ji Dai[1,2,3,4,*]

*Correspondence: hong.wang@siat.ac.cn (H.W.); ji.dai@siat.ac.cn (J.D.)

Received: September 7, 2022; Accepted: November 29, 2022; Published Online: December 5, 2022; https://doi.org/10.1016/j.xinn.2022.100358

GRAPHICAL ABSTRACT

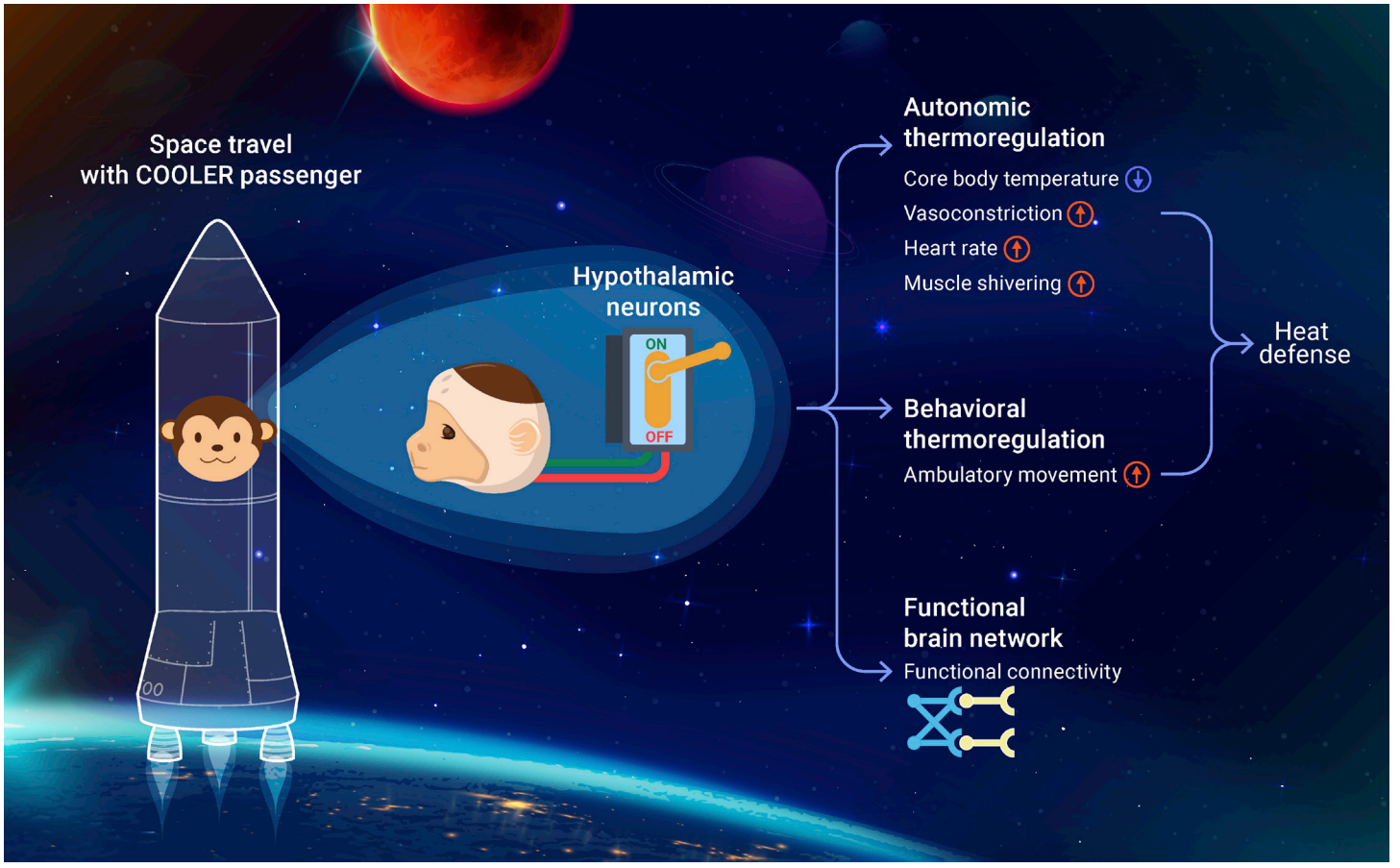

PUBLIC SUMMARY

- Chemogenetic activation of hypothalamic neurons lowers the core body temperature of monkeys.
- Hypothermia is concomitant with a cohort of robust cold-defense behaviors.
- fMRI delineates a brain-wide network as a result of targeted neuronal activation.
- This group of hypothalamic neurons is functionally conserved in rodents and monkeys.
- This is a leap toward human torpor and its application in medicine and space.

ARTICLE

The Innovation

Primate preoptic neurons drive hypothermia and cold defense

Zhiting Zhang,[1,2,6] Liang Shan,[1,2,6] Yuyin Wang,[1,3,6] Wenfang Li,[1] Minqing Jiang,[1] Feng Liang,[1] Shijing Feng,[1] Zhonghua Lu,[1,2,3,4] Hong Wang,[1,2,3,5,*] and Ji Dai[1,2,3,4,*]

[1]CAS Key Laboratory of Brain Connectome and Manipulation, the Brain Cognition and Brain Disease Institute (BCBDI), Shenzhen Institute of Advanced Technology, Chinese Academy of Sciences, Shenzhen 518055, China

[2]Shenzhen-Hong Kong Institute of Brain Science-Shenzhen Fundamental Research Institutions, Shenzhen 518055, China

[3]University of Chinese Academy of Sciences, Beijing 100049, China

[4]Shenzhen Technological Research Center for Primate Translational Medicine, Shenzhen 518055, China

[5]Shenzhen Key Laboratory of Drug Addiction, Shenzhen 518055, China

[6]These authors contributed equally

*Correspondence: hong.wang@siat.ac.cn (H.W.); ji.dai@siat.ac.cn (J.D.)

Received: September 7, 2022; Accepted: November 29, 2022; Published Online: December 5, 2022; https://doi.org/10.1016/j.xinn.2022.100358

Citation: Zhang Z., Shan L., Wang Y., et al., (2023). Primate preoptic neurons drive hypothermia and cold defense. The Innovation **4(1)**, 100358.

Maintaining body temperature within a narrow range is vital for warm-blooded animals. In rodents, the preoptic area (POA) of the hypothalamus detects and regulates core body temperature. However, knowledge about the thermal regulation center in primates remains limited. Here, we show that activating a subpopulation of POA neurons by a chemogenetic strategy reliably induces hypothermia in anesthetized and freely moving macaques. Comprehensive monitoring of physiological parameters reveals that such hypothermia is accompanied by autonomic changes including a rise in heart rate, skeletal muscle activity, and correlated biomarkers in blood. Consistent with enhanced ambulatory movement during hypothermia, the animals show a full range of cold-defense behaviors. Resting-state fMRI confirms the chemogenetic activation of POA and charts a brain-wide network of thermoregulation. Altogether, our findings demonstrate the central regulation of body temperature in primates and pave the way for future application in clinical practice.

INTRODUCTION

For survival, birds and mammals must actively regulate their core body temperatures (Tcores) to remain relatively constant irrespective of the change in ambient temperatures. Dedicated cell types and neural pathways have evolved to regulate Tcores precisely.[1,2] It has been reported that permanent lesions or temporary silencing of the preoptic area (POA) in rats induce failure to maintain Tcores in a hot or cold environment.[3,4] Warming POA locally triggers hypothermia and heat-defensive responses in rats.[5,6] In mice, with the aid of chemogenetic and optogenetic tools, various markers of warm-sensitive neurons (WSNs), which sense peripheral and central temperature changes, have been identified in the POA.[7,8] In 2016, Tan et al. reported that POA neurons co-expressing BDNF/PACAP can be directly activated by ambient warmth. Optogenetic activation of these neurons reduces body temperature in mice and coordinates both autonomic and behavioral thermoregulatory responses.[7] Complementarily, Song et al.[8] identified a heat-sensitive channel, TRPM2, that labels WSNs in the medial POA. Chemogenetic activation of TRPM2-expressing neurons or a subset of VGlut2-expressing neurons drives profound and long-lasting hypothermia in mice.[8] Accumulating data support the notion that POA is a heat-sensing center and that stimulation of this area promotes heat dissipation.

To date, the majority of studies on the neural substrate of thermoregulation use mice as animal models.[9-11] While mice provide an invaluable tool, translating findings from mice to clinical practice is fraught with challenges. For example, mice naturally undergo torpor and tolerate body temperatures as low as 18°C.[12] Their small size and large surface-to-volume ratio permit brisk temperature exchange with the environment. Different from mice, humans and other large animals like nonhuman primates have much weaker tolerance to body temperature changes. For example, both hypothermia (<35°C) and hyperthermia (40.5°C) are medical emergencies.[13] This raises the question of how much humans and rodents have in common regarding neural substrates of thermoregulation. As the closest relative to humans, nonhuman primates (NHPs) can bridge this gap.[14] In baboons and squirrel monkeys, direct cooling or warming of the preoptic/anterior hypothalamus alters body temperature.[15,16] Yet, these experiments do not address cell-type specificity and behavioral responses. It remains unknown if the function of the POA in macaque is evolutionarily conserved as a thermoregulatory center in the brain.

We reason that activating the POA in macaque in a cell-type-specific manner would provide an entry point to understand the thermoregulatory circuit in NHPs and, eventually, humans. Here, we report that chemogenetic stimulation of excitatory neurons in the POA reliably induces hypothermia in macaques. The induced hypothermia in NHPs is accompanied by both autonomic and behavioral responses mediating heat defense, albeit dramatically different from mice. Resting-state functional magnetic resonance imaging (fMRI) scans following the induced hypothermia reveal a brain-wide network of thermoregulation. These findings identify a key role of the POA in thermoregulation in NHPs and shed light on the conserved circuits between rodents and primates.

RESULTS

Chemogenetically activating POA results in hypothermia

To identify whether the POA plays a necessary role in thermoregulation, a chemogenetic strategy was used to manipulate the neural activity of POA. Firstly, adeno-associated virus (AAV), encoding CamKIIα promoter-driven excitatory designer receptor exclusively activated by designer drug (excitatory DREADD, hM3Dq) expression, was bilaterally injected into the POA of two monkeys to express the Gq-coupled DREADD receptors selectively in excitatory neurons.[17] A custom-designed guiding grid mounted on the skull ensured consistent access during MRI scanning and stereotaxic injection (Figure 1A). To achieve reliable and stable Tcore recording, a temperature logger was implanted in the upper abdominal cavity of the experimental monkeys (CM33–EXP/CM34–EXP) and one control monkey (CM53–CON: without virus injection) (Figure 1B). The implanted loggers were programmed to record the temperature every 5 min for months without interfering with the daily activity of the subjects. Ear surface temperatures from these subjects were measured by thermographic imaging (Figure 1C). To monitor the autonomic thermoregulatory responses, electrocardiogram (ECG), electromyogram (EMG), and blood pressure were recorded in restricted animals. Blood samples were taken for a battery of biochemical tests (Figure 1D).

To selectively activate the excitatory neurons expressing hM3Dq in the POA, monkeys were administered with the cognate ligand clozapine-N-oxide (CNO; 10 mg/kg) intramuscularly in their home cages.[18] Saline injections before and after CNO on different days served as controls. Following the injection, subjects were allowed to move freely. The recording by the temperature loggers showed that in two experimental monkeys (CM33–EXP/CM034–EXP), the Tcore decreased quickly following CNO injection (Figures 2A and 2B). We computed the delta Tcore (ΔTc) by subtracting the baseline and found that the mean Tcore between 20 and 240 min after injection decreased by −0.38°C ± 0.02°C (mean ± SE) and −0.49°C ± 0.04°C for subjects CM33–EXP and CM34–EXP, respectively. The operations were repeated four times, and the maximum decreases were 1.32°C and 1.73°C for these two subjects. The saline injection did not induce any change as the mean temperature changes were −0.01°C ± 0.02°C for CM33–EXP ($p < 0.001$, Wilcoxon rank-sum test with the CNO condition) and 0.06°C ± 0.03°C for CM34–EXP ($p < 0.001$). For the control subject that did not receive the virus injection (CM53–CON), CNO induced a minute temperature change (−0.06°C ± 0.03°C; Figure 2C), which was statistically smaller than the drop in either CM33–EXP or CM34–EXP

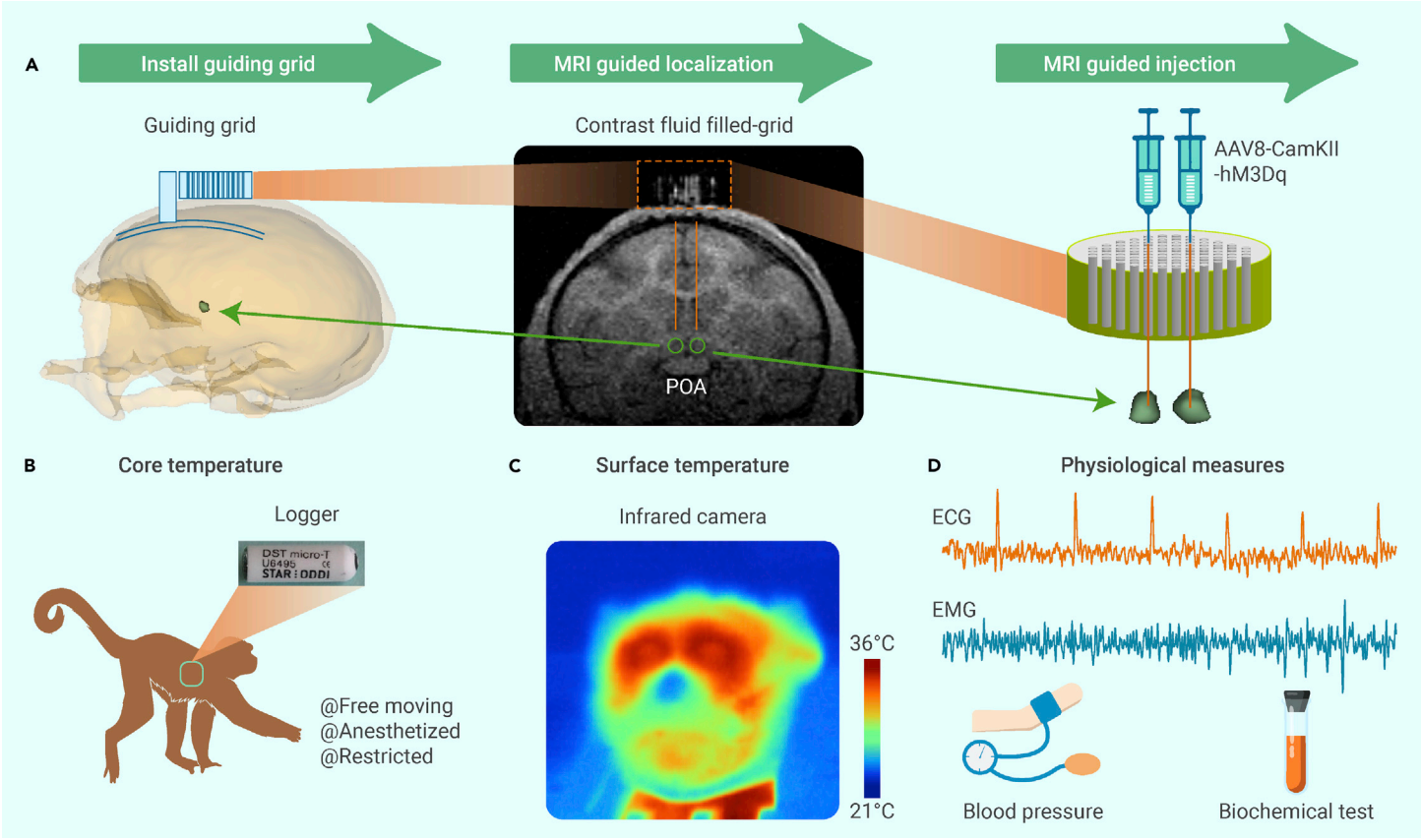

Figure 1. Illustration of experimental setups in macaques (A) A custom-designed guiding grid was used to guide the injection of virus AAV8-CamKII-hM3Dq into bilateral POAs following MRI scans. **(B)** A piece of temperature logger was implanted in the abdominal cavity to automatically record the Tcore for the long term. **(C)** An infrared camera was used to capture the surface temperature of experimental animals. **(D)** Multiple measures including ECG, EMG, blood pressure, and biochemical tests of blood samples were used to monitor physiological states.

($p < 0.01$). Therefore, CNO alone does not alter the Tcore. We conclude that the hypothermia in the experimental subjects was caused by CNO binding to the DREADD receptor.

As ambulatory movement greatly influences Tcores, we sought to remove this factor by studying anesthetized animals. During the anesthesia, the subjects' Tcore increased following saline injection (blue lines in Figures 2D–2F) since they were warmed by an external heat source. Interestingly, CNO injections slowed down the rise of the Tcore in two experimental monkeys compared with saline treatment (red lines in Figures 2D and 2E), whereas the control monkey showed an identical rise of Tcore after saline and CNO injections. (Figure 2F). This phenomenon suggests that chemogenetic activation of POA neurons antagonizes external warming, presumably by lowering the Tcore. In summary, chemogenetic activation of POA neurons during both freely moving and anesthetized NHPs reliably triggers hypothermia in the experimental group.

Chemogenetically activating POA enhanced locomotion

Behavior is a critical component of thermoregulation. Increasing or inhibiting ambulatory movement is one strategy to boost or curb heat production. For humans, one effective way to defend body temperature against cold is to exercise and generate heat (e.g., running).[1] In rodents, stimulation of WSNs in the POA results in hypothermia and concomitant cold-seeking behaviors.[7] Since we have observed reliable hypothermia in the two experimental subjects, we next set to identify their behavioral responses. To quantify behavior, subjects were permitted to explore an observing cage made of toughened glass walls. The movement traces were captured by video cameras of a commercial analysis system and analyzed by custom codes.[19] Both CM33–EXP and CM34–EXP traveled longer distances after CNO injection than saline within a trial of 3 h (Figures 3A and 3B). Quantitative analysis indicated that the total moving distance within the 3 h after CNO injection was dramatically longer than that of saline injection ($p < 0.001$ for CM33 and $p < 0.01$ for CM34, paired t test; Figures 3C and 3D). As a control, for CM53–CON, CNO administration did not induce any alteration in moving distance ($p > 0.5$; Figure 3E). In brief, CM033–EXP/034–EXP both decreased the Tcore and raised the ambulatory movement after CNO. The control group (CM53–CON) did not.

Autonomic thermoregulation changes in restricted animals

We hypothesized that increasing movement generated heat and compensated for heat loss during hypothermia. If so, restricting movement may preclude animals from generating additional heat and should further decrease the Tcores in CM33–EXP and CM34–EXP.

To test this hypothesis, we habituated the experimental group (CM33/CM34) in restriction. Since the control animal (CM53) did not demonstrate DREADD-dependent hypothermia, it was excluded in the experiment under restriction. Under restriction, surface temperatures, ECG, EMG, and blood pressure were monitored for 3 h after CNO or saline injection. Similar to freely behaving animals, the Tcore decreased quickly following CNO administration for both monkeys. Under restriction, the Tcore decreased by $-0.69°C \pm 0.03°C$ and $-0.91°C \pm 0.03°C$ compared with saline injections (Figures 4A and 4B). When comparing the hypothermia in restricted animals with the freely behaving condition, the decrease of the Tcore is greater when the ambulatory movement is prohibited ($0.38°C \pm 0.02°C$ and $0.49°C \pm 0.04°C$; Figures 2A and 2B). Thus, these results suggest that chemogenetic stimulation of the POA reliably reduced Tcores in restricted animals, consistent with the effect in the freely behaving condition. Thus, limiting ambulatory movement potentiated the magnitude of hypothermia.

In mice, stimulation of WSNs in the POA promotes heat loss by lowering the surface temperatures in the trunk and increasing the surface temperatures in the tail by vasodilation.[8] We found that the glabrous skin of the monkey ear is accessible for consistent thermographic imaging. As illustrated in Figures 4C and 4D, the surface temperatures of the ears for CM33 and CM34 decreased following CNO injections (red). There was no noticeable change of the ear surface temperature upon saline injection neither 1 day before (light blue) nor 3 days after (blue) CNO condition.

Concurrent with hypothermia, the heart rate increased robustly for both monkeys by 40–60 bpm (red lines in Figures 5A and 5B) within the recording

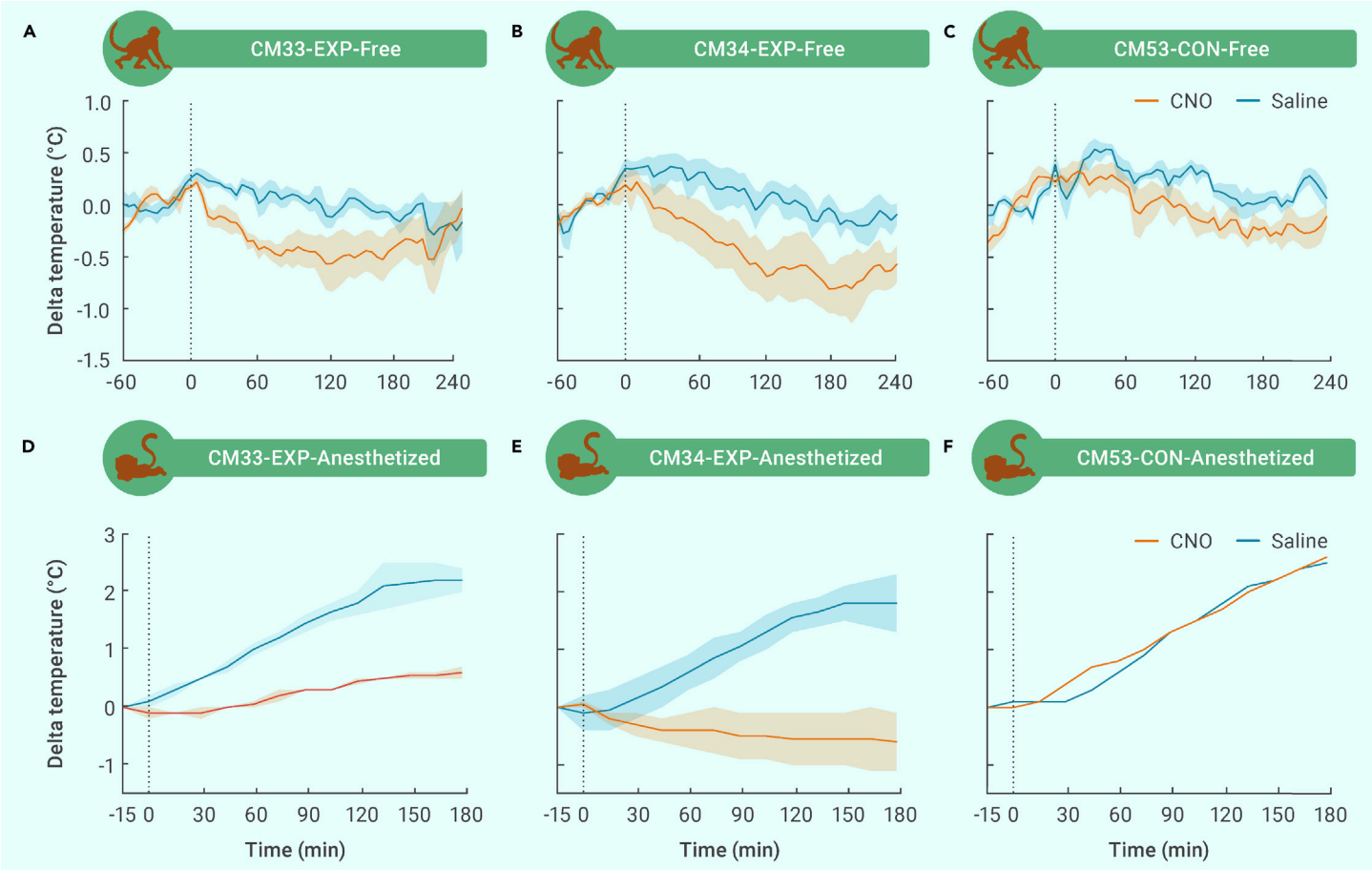

Figure 2. Chemogenetic activation of excitatory neurons in the POA induced hypothermia in both freely behaving and anesthetized animals (A–C) The delta temperature compared with baseline for two experimental subjects (CM33–EXP and CM34–EXP) and one control subject (CM53–CON) during freely behaving, of which the x and y axes indicate time and the delta temperature. Zeros in the x axis indicate injection time, and blue and red represent saline and CNO administration, respectively. Shadows indicate SEM. **(D–F)** The delta temperature for three subjects when they were anesthetized. Red: CNO; blue: saline.

intervals. Saline injections did not generate a comparable effect (blue lines in Figures 5A and 5B). On the other hand, while blood pressure was also measured every 5 min, we did not notice any consistent effect across these subjects (Figure S1). Interestingly, EMG recordings from surface electrodes on the hindlimbs showed multiple transient ripple-like signals after CNO injection, which contained higher power in frequency bands under 40 Hz than in saline conditions (Figures 5C and 5D). Low-frequency signals in EMG have been correlated with muscle shivering.[20] Enhanced ambulatory movement, heart rate, and muscle shivering support that CNO-induced hypothermia results in cold defense through both behavioral and autonomic thermoregulatory means.

In line with these EMG findings, biochemical tests of blood samples taken from these subjects confirmed robust increases of creatine kinase (Figure 5E) and myoglobin (Figure 5F) in response to CNO administration (see Tables S1–S3 for the full list of all tested biomarkers), which were temporary and returned to normal 3 days later. Strenuous exercises boost heart rate, the blood level of creatine kinase, and myoglobin, as well.[1,21,22] We reason that the cold-defense component of thermoregulation in NHPs mimics strenuous exercises. As a consequence, an increase in the amylase level (Figure 5G) may indicate hyperactivity of the pancreas to balance blood sugar.

Network effects revealed by fMRI

To evaluate the neural responses to chemogenetic activation of the POA at the whole-brain scale, subjects underwent fMRI scans after CNO administration under general anesthesia. Parameters such as regional homogeneity (ReHo), the amplitude of low-frequency fluctuation (ALFF), fractional ALFF (fALFF), and functional connectivity (FC) were computed to quantify resting-state fMRI signals. By manually selecting the POA as the region of interest (ROI) from structural images (Figure 6A), the ReHo signals of the POA for different subjects are shown in Figure 6B. The ReHo of the POA quickly rose within 10 min after CNO administration in both CM33 and CM34 and maintained a high level throughout the recording period compared with control CM53. Time-dependent elevation of ReHo in the POA after CNO administration strongly supports the successful chemogenetic activation in POA neurons. For other ROIs adopted from the atlas (112RM-SL),[23] the mean ReHo values of all ROIs (n = 22) calculated in the standard space for CM33 and CM34 were both stronger than CM53 ($p < 0.001$, paired t test; Figure 6C), indicating a general activation of the brain as a consequence of POA stimulation.

The temporal dynamics of ReHo for many ROIs recapitulates the change of ReHo in the POA (Figure 6D), particularly parietal regions including the inferior parietal lobule (IPL; bold green lines), parietal lobe (PL; bold blue lines), and primary somatosensory cortex (S1; bold purple lines). Given the well-documented functions of these regions in multisensory integration,[24-26] such activation reflects the possibility that the animals have detected the change of the Tcore. The ALFF/fALFF did not show notable differences (Figure S2).

FC is defined by measuring the similarity between brain signals arising from two regions.[27] It reveals FC between two brain areas. The FC analysis uncovered broad connections between brain regions in CM33 and CM34 compared with CM53 (Figure 6E), of which warm and cold colors indicate positive and negative FC, respectively. Taking CM53 as a reference, the relative FCs of CM33 and CM34 are illustrated in Figure 6F. Some connections remain surprisingly consistent between CM33 and CM34, for example, the FCs between the IPL and superior temporal sulcus, the insular cortex (IC) and S1, and the circular sulcus (CS) and PL. To better visualize the consistent changes, we ranked the mean relative FC in both CM33 and CM34 (Figure 6G). On average, the CS together with the nearby IC showed the largest relative FC, which agrees with the role of the IC as the interoception center, including detecting the heartbeat, discomfort, and temperature.[28-30]

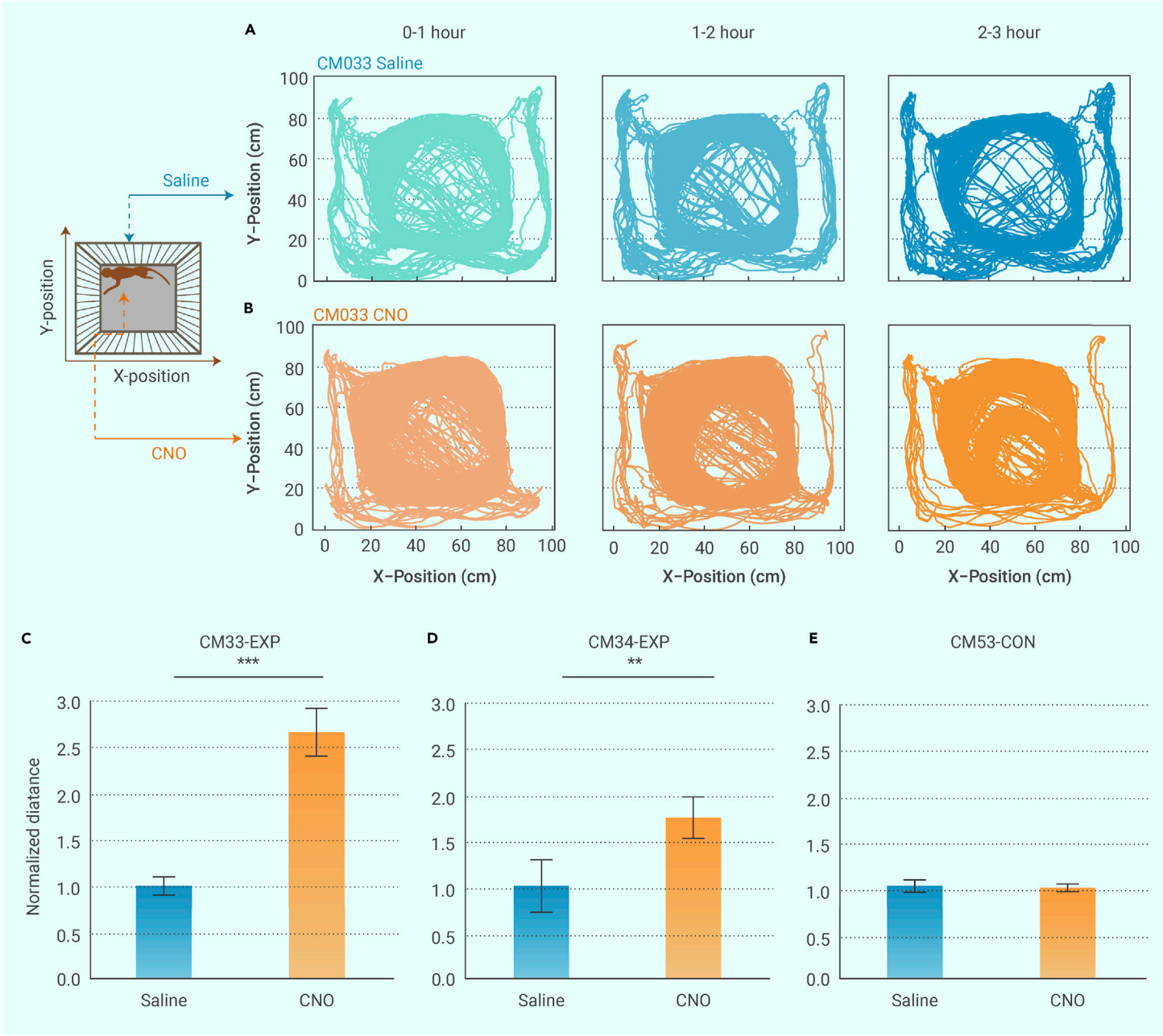

Figure 3. CNO-induced hypothermia is concurrent with increased ambulatory movement (A and B) The moving trajectory in an observing cage for subject CM33 after receiving saline or CNO injection. x and y positions correspond to the horizontal and vertical axes of the observing cage from the top view. Each column represents the trajectory in that hour as indicated on top. **(C–E)** The mean of normalized moving distance in six consecutive half-hours for experimental and control subjects after receiving saline (blue) or CNO (magenta) injection. Error bars indicate standard error. ***p < 0.001; **p < 0.01.

In summary, resting-state fMRI analysis confirmed the specific activation of the POA and discovered several functional connections in the brain. Of note, the interoception center IC and nearby regions feature among the strongest connections.

DISCUSSION

The POA has long been believed to be the thermoregulatory center of the brain. A set of molecular markers have been identified in the POA to label the WSNs in mouse brains. Stimulation of WSNs triggers heat loss and hypothermia in mice. We have shown that activating excitatory neurons in the POA by chemogenetic techniques reliably induces hypothermia in conscious and anesthetized macaques. This is one of the few cases where chemogenetic manipulation results in robust behavioral and autonomic changes. Similar to mice, POA neurons coordinate both behavioral and autonomic thermoregulatory responses. In contrast to the mouse model, POA activation promotes an increase in ambulatory movement, vasoconstriction, heart rate, and muscle shivering, all pointing to a cold-defense mechanism. Resting-state fMRI unmasked a local circuit in the IC, consistent with its central role in interoception for temperature, heart rate, and comfort.

Our findings reveal both common and species-specific roles of the POA as the thermoregulatory "heat loss" center. We probe the basis of thermoregulation in humans and pave the way for future translational studies from bench to bedside. With the growing passion for human spaceflight,[31,32] our hypothermic monkey model is a milestone on the long path toward artificial hibernation.

Activation of excitatory neurons in POA drives hypothermia in NHPs

Opto- and chemogenetic studies in combination with cell-type-specific driver lines in mice have revealed a causal relationship between genetically defined neurons and their functions. However, due to the paucity of equivalent driver lines in NHPs, there is currently no such strategy to dissect cell type labeled by molecular markers and their roles in the nervous system. An alternative approach is to

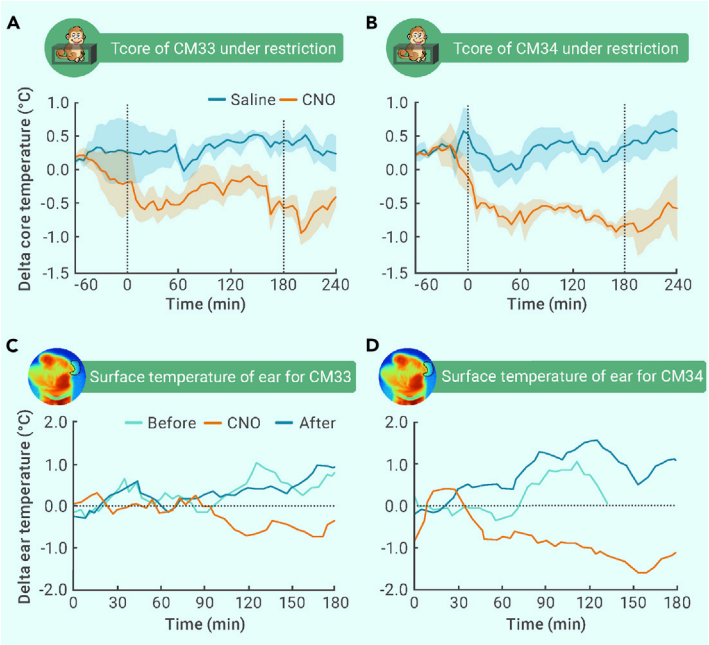

Figure 4. The temperature changes following saline and CNO administration when the subjects were restricted (A and B) The delta core temperature compared with the baseline for subjects CM33 and CM34 when they were restricted in a monkey chair. Blue and red represent saline and CNO conditions, respectively, with shadows indicating the SEM. The first dashed line indicates the time of injection, and the second dashed line indicates the end of restriction. **(C and D)** The delta of ear temperature adopted from infrared images for CM33 and CM34 (as indicated by the inset). Red represents CNO condition, and light blue and blue represent saline injection 1 day before and 3 days after CNO.

package cell-type-specific promoters driving the expression of opto- or chemogenetic receptors in AAV. Using AAV encoding tyrosine hydroxylase promoters driving the expression of channelrhodopsins, Stauffer and colleagues succeeded in manipulating dopaminergic neurons in NHPs.[33] Here, by restricting the expression of Gq-DREADD receptor with CamKII promoter, we primarily target the excitatory neurons subset of the POA in wild-type macaques.

The POA is a highly heterogeneous area. Thus, this method is especially necessary to limit the group of neurons activated by CNO administration. Early studies report that cooling or heating the anterior hypothalamus of NHPs alters body temperatures.[15,16] By introducing a chemogenetic tool with a cell-type-specific promoter, we achieve unprecedented cell-type specificity in the field of thermoregulation in NHPs. In mice, Song et al.[8] report that chemogenetic stimulation of 20% of excitatory neurons (VGlut2+) is sufficient to drive Tcores as low as 28°C in mice. Consistent with this finding, chemogenetic activation of excitatory neurons (CamKII promoter driving) in the POA also induces hypothermia in macaques, albeit to a smaller extent than in rodents. Our discovery supports that the excitatory neurons in the POA are evolutionarily conserved in both their molecular identity and function.

Limited by the number of animals and spatial resolution of MRI, neither can we identify the subnuclei localization of the viral expression nor can we exclude the neighbor area of the POA from vial leakage. In the vicinity of POA, the bed nucleus of the stria terminalis and the paraventricular nuclei of the hypothalamus have been implicated as the autonomic and neuroendocrine centers in rodents.[34] Recent studies in mice have shown that chemogenetic activation of Brs3+ neurons in the paraventricular nuclei of the hypothalamus increases the Tcore instead and, in the bed nucleus of the stria terminalis, does not alter the Tcore.[35,36] Taken together, in mice, among nearby regions, the POA is the key area capable of triggering heat loss upon chemogenetic activation.

POA neurons orchestrate behavioral and autonomic thermoregulation in NHPs

In mice, activation of WSNs in the POA induces behavioral changes including immobility and cold-seeking behavior, as well as autonomic alterations such as bradycardia.[7,8] All of the thermoregulatory outcomes are orchestrated to facilitate hypothermia. On the contrary, in NHPs, stimulation of the POA evokes behavioral and autonomic cold defense: increasing ambulatory movement, enhanced vasoconstriction, muscle shivering, and tachycardia. Collectively, all responses combat the chemogenetically induced hypothermia. This provides one explanation for a reduced magnitude of hypothermia in NHPs compared with rodents. Another plausible interpretation is that certain neural pathways have evolved in primates to safeguard the Tcore and that this mechanism is missing in rodents. This hypothesis is supported by the fact that in primates, only a small deviation of Tcores can be well tolerated, while mice can survive torpor with a Tcore as low as 18°C. The lack of comparative studies of thermoregulatory mechanisms between rodents and primates, both at anatomical and functional levels, warrants further study. Besides, the seeming milder hypothermia in NHPs may arise from the relatively low efficacy of DREADD-based chemogenetic activation.

fMRI delineates a thermosensory network in the brain

Activation of POA neurons in monkeys results in hypothermia and concomitant changes in discrete brain areas revealed by fMRI scanning. Of them, we notice broad functional connections of the limbic system, including the IC, CS, hippocampus, and parahippocampal gyrus. All of the above are related to processing perception and emotional information. For example, the IC is the hub of interoception, mediating the perception of temperature and heart rate. The synaptic activity of the hippocampus is temperature dependent.[37,38] We reason that the monkeys perceive the change of a Tcore of less than 1°C with high accuracy and, in return, coordinate a battery of cold-defense behaviors. Chemogenetic manipulation together with fMRI offers a means to begin to investigate the causal relationship between defined cell types and their influence over the entire brain.

The effect of anesthesia on body temperature regulation

During general anesthesia, thermoregulation is impaired, and hypothermia commonly happens.[39] For instance, during anesthesia, not only the sensory inputs but also the motor outputs together with sympathetic functions are shifted toward inhibition.[40] Therefore, under general anesthesia, the animals are unlikely to recruit thermoregulatory effector organs, such as skeletal muscles, let alone perform cold-defense behaviors. Studies on humans indicate that the body temperature declines at a low speed of 0.5°C–1°C/h when exposing the body to a cold operating room environment and undergoing cold surgical skin prep solutions.[39] In this study, recording conditions were kept constant between sessions, such as anesthesia depth and external heating. Yet, we detect strictly DREADD-dependent antagonism of external warming. In addition, fMRI analysis indicates that anesthesia does not induce ReHo signals in the control group equivalent to the experiment group, and neither does the FC. To summarize, though anesthesia confounds thermoregulation, activating the POA initializes heat loss.

MATERIALS AND METHODS

Animals

Three cynomolgus monkeys (*Macaca fascicularis*) (male, 1–3 years old, weight 2–2.3 kg) were involved in the study (please be advised that we were not able to perform experiments on more subjects due to the shortage of experimental monkeys). All monkeys were housed in a primate facility accredited by The Association for Assessment and Accreditation of Laboratory Animal Care with environmental control (ambient temperature: 24°C ± 1°C, relative humidity: 50% ± 5%), where they received sufficient food, water, and professional veterinary care. All experiments were performed under ambient temperature. All experimental procedures were approved by the Institutional Animal Care and Use Committee at Shenzhen Institutes of Advanced Technology, Chinese Academy of Sciences (approved case ID: SIAT-IACUC-200103-NS-WH-A0999) following the guidelines stated in the Guide for Care and Use of Laboratory Animals (eighth edition, 2011).

Surgeries and virus injections

All surgical procedures were performed using sterile methods while the subject was anesthetized. For general anesthesia, monkeys were first administered atropine (0.05 mg/kg, intramuscular) to decrease bronchial secretions, and then ketamine (15 mg/kg, intramuscular) and propofol (6 mg/kg, intravenous) were given successively to induce and maintain anesthesia. A standard operating table with constant heating was used to place the subjects. ECG, heart rate, oxygen saturation (SpO2), blood pressure, and rectal temperature were continuously monitored (Mindray, uMEC7).

Virus injections were performed on three monkeys to express Gq receptor (AAV2/9-CamKIIa-hM3Dq-mCherry, titer 1.86 × 10^{13}, purchased from TaiTool) in the POA, and one

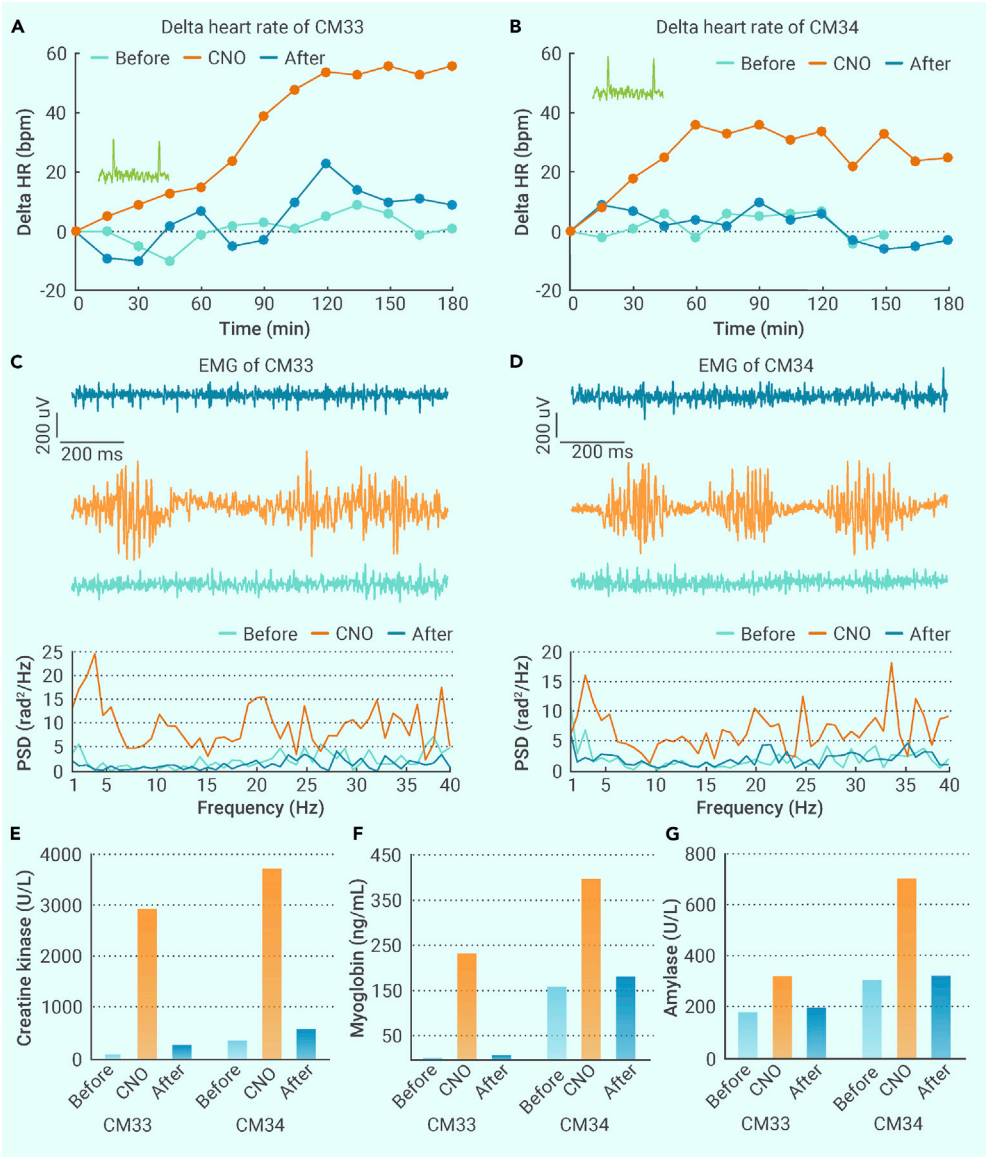

Figure 5. Autonomic responses of heart rate and muscle activity after CNO administration (A and B) The delta heart rate following injection of CNO or saline for CM33 and CM34. Red represents CNO condition, and light blue and blue represent saline injection 1 day before and 3 days after CNO. **(C and D)** Typical EMG signals and corresponding power spectra in CNO and saline conditions for CM33 and CM34. **(E–G)** The level of creatine kinase, myoglobin, and amylase in blood in saline and CNO conditions for two subjects.

monkey (CM53–CON) receiving no virus injection served as a control. For monkeys CM33–EXP and CM34–EXP, a grid with multiple guide holes was installed vertically above the POA, and then the accurate coordinates for the injection could be obtained through the guide grid after the MRI scan. A 3T scanner with 0.5 mm resolution for T1-weighted images was used for all MRI scans (3T Tim Trio scanner, Siemens). An MPRAGE sequence with parameters TR/TE = 2,100/3.18 ms, TI = 1,100 ms, flip angle = 8, and matrix = 320 × 320 was used to generate 240 slices.

The virus injection was performed following the procedures that have been described in detail elsewhere.[41,42] In brief, a total volume of 6 μL virus was bilaterally injected into the POA at the speed of 200 nL/min (WPI, Micro4, UMP3) using a cemented syringe and needle (Hamilton, 80208). After lowering the needle to the target depth, we waited 10 min to allow the tissue to stabilize before starting the injection. After the injection was finished, an extra 10 min of waiting time was given to allow the virus to spread before retracting the needle.

To continuously record the body core temperature, a temperature logger (STAR-ODDI, micro-T) was implanted inside the abdominal cavity and fixed to the abdominal wall for each monkey following standard surgical procedures. To avoid any acute response due to the surgery, at least 2 weeks were given for the subject to recover before the temperature recording experiment. The logger was taken out via another surgery after all recording sessions were completed, and the abdominal cavity was sutured for the subject to recover.

Temperature recordings

The body core temperature was recorded by the implanted logger for all monkeys before and after CNO/saline administration (CNO dihydrochloride, Hellobio, 10 mg/kg, intramuscular injection). The logger was set to record every 5 min during the recording. Saline and CNO were injected on different days, and two CNO injections were separated for at least 7 days. The recording was conducted while the monkeys were moving freely or restrained in a monkey chair. For the freely moving condition, the subjects were housed in their home cages. The period 60 min before CNO/saline injection was taken as the baseline to calculate ΔTc. For the in-chair condition, the subjects were taken out from their home cages and restrained in a custom-made chair so that they can only make minor movements. Since these operations may induce variation in Tc, an earlier period (−120∼−60 min before injection) was used as the baseline to calculate ΔTc.

For temperature recording during anesthesia, the animal was first anesthetized using the procedures described above, with the heart rate, blood pressure, and respiration continuously monitored, and then the animal was placed on an electrothermal pad and wrapped with a blanket. The anesthetic level was adjusted to ensure that toe-pinch reflexes and corneal reflexes were consistently absent. The rectal temperature was recorded from a thermal sensor that was placed inside the anus (Mindray, uMEC7) for 3 h. The period 15 min before CNO/saline injection was taken as the baseline.

For surface temperature measurement, the monkey was sitting in front of the thermal camera (Fluke TiX580), which was fixed on a tripod. Therefore, the distance and the viewing angle can keep relatively consistent throughout the recording sessions. A thermographic image was taken every 5 min simultaneously with a light image. To obtain the mean temperature of the ear, the contour of the ear was manually selected from the infrared images and analyzed by SmartView software (v.4.1.43.0).

Physiological recording and analysis

ECG and EMG were recorded using a physiological signal acquisition system (TECHMAN, HPS-102) for subjects under restriction. Before the experiments, they were habituated to the chair and recording room for at least 180 min on three separate days. The experiment was conducted by the same experimenters in the same environment and at the same time on different days. During the experiment, ECG and EMG signals were continuously recorded for at least 180 min at a sampling rate of 500 and 1000 Hz, respectively. The subjects did not need to perform any task but sat quietly in the chair with a small amount of water and treats received.

The heart rate was extracted from ECG signals using the e-MOUSE software (Mouse Specifics). Specifically, the raw signals were equidistantly divided into 15 min segments, from which a 30 s stable piece was selected for heart rate analysis. The heart rate during the 15 min before injection was taken as the baseline. EMG signals were visually examined throughout the time course, and the ripple-like signals were manually selected for further power spectrum analysis.

Blood samples were collected 40–50 min after CNO/saline injections during the same physiological recording session when the subjects were restricted. Then, blood routine measures (Mindray, BC-5180CRP), biochemical measures (MNCHIP, Pointcare V3; Wondfo, FS-205), and electrolyte measures (EDAN, i15 VET) were performed following procedures recommended by the manufacturers.

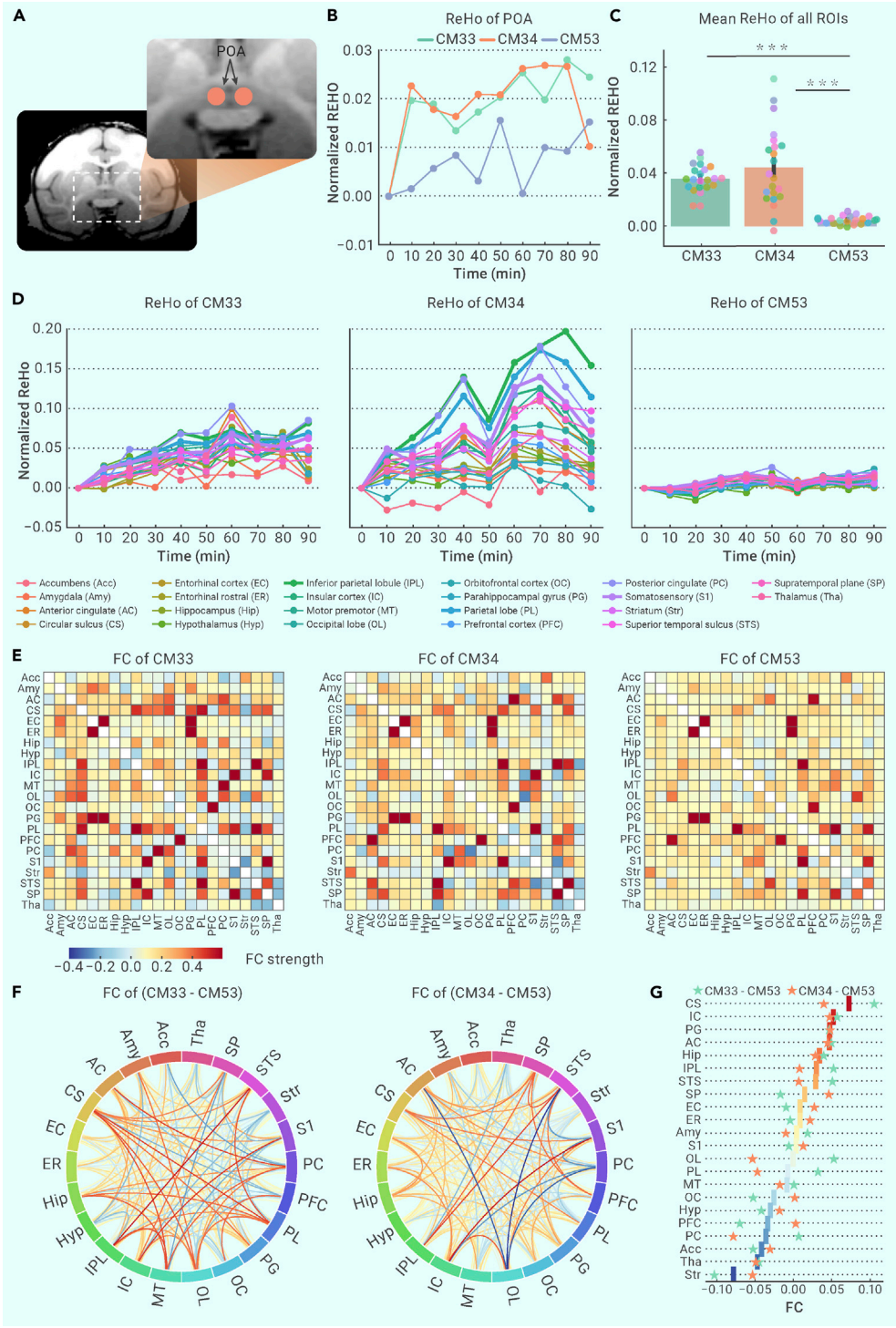

Figure 6. The results of resting fMRI scans following intramuscular CNO injection (A) The illustration of ROI selection for the POA. **(B)** The ReHo dynamics of the POA for three subjects during 90 min after CNO injection. **(C)** The mean ReHo of all included ROIs for three subjects. ***p < 0.001. **(D)** The temporal dynamics of ReHo for all included ROIs after CNO injections for three subjects. **(E)** The functional connectivity (FC) between all ROIs for three subjects. The color bar indicates the FC strength. **(F)** The relative FC strength for CM33 and CM34 compared with CM53. **(G)** The mean of relative FC for each ROI. Green and yellow asterisks represent CM33 and CM34, respectively.

Locomotion recording and analysis

A custom-made observing cage (100 × 100 × 100 cm) located in a designated recording room was used to record the effect of CNO injection on freely behaving animals. The top and front sides of the cage were made of toughened glass to allow direct video recording, and two cameras recorded the top view (x and y dimensions) and side view (x and z dimensions), respectively. A commercial system (ViewPoint, Vigie Primate), which has been used to analyze motion behaviors in other studies using primates,[19] was used to analyze the subject's activity and extract movement data from the recorded videos. The sample rate for video tracking was 25 Hz synchronously for both the top view and the side view. The tracking data were normalized to 0–100 cm for all x, y, and z axes, of which x represents right to left, y represents front to back, and z represents bottom to top. Monkeys were transferred from their home cages to the observing cage and recorded individually with a small amount of water and treats provided. Before the experiments, all monkeys have been habituated to the observing cage by placing them inside for at least 1 h on three separate days. During the experiments, videos capturing the subjects' behavior were recorded for at least 180 min. The moving trajectories were reconstructed and quantified from the recorded data using custom codes.

To quantify the difference in moving distance between saline and CNO conditions, the moving distance was first extracted for each 30 min segment, generating six data points for saline and CNO conditions, and then all data points were normalized by the mean of saline condition. Statistical analysis was performed by paired t test.

fMRI scan and data analysis

The subject was anesthetized following the procedures described above. The BOLD signal was obtained by a 3T scanner (3T Tim Trio scanner, Siemens) using a general setting (gradient echo, echo-planar imaging, TR (repetition time) = 3,000 ms, TE (echo time) = 30 ms, flip angle = 90, slice thickness = 1.5 mm). A baseline scan was run before the CNO injection (10 mg/kg, intramuscular), and then the scan was repeated every 10 min nine times following the CNO injection.

Resting-state fMRI data were preprocessed with a Matlab-based toolbox DPARSFA (http://rfmri.org/DPARSF).[23] In brief, data were first transformed from DICOM into NIFTI format. Slice timing and realignment were performed after removing the first five time points. Each T1 structural image was extracted and co-registered to the functional images, which were then normalized into the 112RM-SL template (the default monkey brain template in DPARSFA) using the T1 image unified segmentation module and resampled into a voxel size of 2 × 2 × 2 mm.

A total of 23 ROIs were used in this study, of which 22 were taken from the Paxinos_composite subdirectory (http://brainimaging.waisman.wisc.edu/~converse/rhesusROIs/) and aligned to the 112RM-SL template (i.e., standard space ROIs). The 23rd was the POAs and was manually created as pairs of spherical ROIs for each monkey based on the T1 structural image in individual space.

After preprocessing, the following indicators were calculated, and the values of each ROI were extracted for further statistical analysis:

(1) mReHo: ReHo calculation was performed using Kendall's coefficient of concordance to measure the synchronicity of the time series between a given voxel with its 26 nearest neighbors in a voxel-wise way.[43] After detrending and bandpass filtering (0.01–0.1 Hz), the Kendall's coefficient of concordance map was generated for each datum and was divided by the global mean value to obtain the mReHo map. Smoothing was performed using a 2 mm FWHM Gaussian kernel for the results. The mReHo values of 22 ROIs in standard space were extracted and baseline corrected by subtracting the preinjection value.

(2) mALFF/mfALFF: the ALFF/fALFF were believed to reflect the spontaneous fluctuations and the functional activities of the brain.[44] To compute the ALFF, spatial

smoothing was first performed on the data with a 2 mm FWHM Gaussian kernel. The time series were converted to the frequency domain using a fast Fourier transform to obtain the power spectrum. The square root of the power spectrum was calculated and then averaged across 0.01–0.1 Hz at each voxel; the ALFF was then generated. To obtain fALFF, the sum of the amplitude across 0.01–0.1 Hz was divided by that of the entire frequency range. To further obtain the mALFF/mfALFF, all ALFF/fALFF maps were divided by their mean value. Finally, the mALFF/mfALFF values of the 22 standard ROIs were extracted and baseline corrected by subtracting the preinjection value.

(3) FC: FC analysis was carried out by applying an ROI-based approach. Briefly, spatial smoothing (2 mm FWHM Gaussian kernel), detrend, and nuisance covariates regression were first performed in each datum to improve the signal-to-noise ratio. Band-pass filtering (0.01–0.1 Hz) was applied to remove spurious fluctuations in FC.[45] The averaged time course was obtained for each ROI, and the pairwise correlation coefficients were calculated to indicate the strength of FC between each pair of ROIs and then baseline corrected by subtracting the preinjection value.

For the POA, the computations of mReHo, mALFF/mfALFF, and FC were conducted similarly as described above except that all values were extracted in the individual space rather than the standard space.

REFERENCES

1. Morrison, S.F. (2016). Central neural control of thermoregulation and brown adipose tissue. Auton. Neurosci. ***196***, 14–24.
2. Morrison, S.F. (2016). Central control of body temperature. F1000Res. ***5***, 880.
3. Abbott, S.B.G., and Saper, C.B. (2017). Median preoptic glutamatergic neurons promote thermoregulatory heat loss and water consumption in mice. J. Physiol. ***595***, 6569–6583.
4. Ishiwata, T., Saito, T., Hasegawa, H., Yazawa, T., Kotani, Y., Otokawa, M., and Aihara, Y. (2005). Changes of body temperature and thermoregulatory responses of freely moving rats during GABAergic pharmacological stimulation to the preoptic area and anterior hypothalamus in several ambient temperatures. Brain Res. ***1048***, 32–40.
5. Carlisle, H.J. (1966). Behavioural significance of hypothalamic temperature-sensitive cells. Nature ***209***, 1324–1325.
6. Carlisle, H.J., and Laudenslager, M.L. (1979). Observations on the thermoregulatory effects of preoptic warming in rats. Physiol. Behav. ***23***, 723–732.
7. Tan, C.L., Cooke, E.K., Leib, D.E., Lin, Y.C., Daly, G.E., Zimmerman, C.A., and Knight, Z.A. (2016). Warm-sensitive neurons that control body temperature. Cell ***167***, 47–59.e15.
8. Song, K., Wang, H., Kamm, G.B., Pohle, J., Reis, F.d.C., Heppenstall, P., Wende, H., and Siemens, J. (2016). The TRPM2 channel is a hypothalamic heat sensor that limits fever and can drive hypothermia. Science ***353***, 1393–1398.
9. Morrison, S.F., and Nakamura, K. (2011). Central neural pathways for thermoregulation. Front. Biosci. ***16***, 74–104.
10. Tan, C.L., and Knight, Z.A. (2018). Regulation of body temperature by the nervous system. Neuron ***98***, 31–48.
11. Tansey, E.A., and Johnson, C.D. (2015). Recent advances in thermoregulation. Adv. Physiol. Educ. ***39***, 139–148.
12. Hrvatin, S., Sun, S., Wilcox, O.F., Yao, H., Lavin-Peter, A.J., Cicconet, M., Assad, E.G., Palmer, M.E., Aronson, S., Banks, A.S., Griffith, E.C., and Greenberg, M.E. (2020). Neurons that regulate mouse torpor. Nature ***583***, 115–121.
13. Cheshire, W.P., Jr. (2016). Thermoregulatory disorders and illness related to heat and cold stress. Auton. Neurosci. ***196***, 91–104.
14. Putnam, P.T., Young, L.J., and Gothard, K.M. (2018). Bridging the gap between rodents and humans: the role of non-human primates in oxytocin research. Am. J. Primatol. ***80***, e22756.
15. Gale, C.C., Mathews, M., and Young, J. (1970). Behavioral thermoregulatory responses to hypothalamic cooling and warming in baboons. Physiol. Behav. ***5***, 1–6.
16. Laudenslager, M.L. (1976). Proportional hypothalamic control of behavioral thermoregulation in the squirrel monkey. Physiol. Behav. ***17***, 383–390.
17. Roth, B.L. (2016). DREADDs for neuroscientists. Neuron ***89***, 683–694.
18. Upright, N.A., Brookshire, S.W., Schnebelen, W., Damatac, C.G., Hof, P.R., Browning, P.G.F., Croxson, P.L., Rudebeck, P.H., and Baxter, M.G. (2018). Behavioral effect of chemogenetic inhibition is directly related to receptor transduction levels in rhesus monkeys. J. Neurosci. ***38***, 7969–7975.
19. Charvin, D., Di Paolo, T., Bezard, E., Gregoire, L., Takano, A., Duvey, G., Pioli, E., Halldin, C., Medori, R., and Conquet, F. (2018). An mGlu4-positive allosteric modulator alleviates Parkinsonism in primates. Mov. Disord. ***33***, 1619–1631.
20. Blondin, D.P., and Haman, F. (2018). Shivering and nonshivering thermogenesis in skeletal muscles. Handb. Clin. Neurol. ***156***, 153–173.
21. Kindermann, W. (2016). Creatine kinase levels after exercise. Dtsch. Arztebl. Int. ***113***, 344.
22. Sabriá, M., Ruibal, A., Rey, C., Foz, M., and Domenech, F.M. (1983). Influence of exercise on serum levels of myoglobin measured by radioimmunoassay. Eur. J. Nucl. Med. ***8***, 159–161.
23. Chao-Gan, Y., and Yu-Feng, Z. (2010). DPARSF: a MATLAB toolbox for "Pipeline" data analysis of resting-state fMRI. Front. Syst. Neurosci. ***4***, 13.
24. Feher, J. (2012). 4.3 - Cutaneous sensory systems. In Quantitative Human Physiology, Second Edition, J. Feher, ed. (Academic Press), pp. 389–399.
25. Maravita, A., and Romano, D. (2018). Chapter 25 - the parietal lobe and tool use. In Handbook of Clinical Neurology, G. Vallar and H.B. Coslett, eds. (Elsevier), pp. 481–498.
26. Sereno, M.I., and Huang, R.S. (2014). Multisensory maps in parietal cortex. Curr. Opin. Neurobiol. ***24***, 39–46.
27. Shan, L., Huang, H., Zhang, Z., Wang, Y., Gu, F., Lu, M., Zhou, W., Jiang, Y., and Dai, J. (2022). Mapping the emergence of visual consciousness in the human brain via brain-wide intracranial electrophysiology. Innovation ***3***, 100243.
28. Benarroch, E.E. (2019). Insular cortex: functional complexity and clinical correlations. Neurology ***93***, 932–938.
29. Gogolla, N. (2017). The insular cortex. Curr. Biol. ***27***, R580–R586.
30. Craig, A.D., Chen, K., Bandy, D., and Reiman, E.M. (2000). Thermosensory activation of insular cortex. Nat. Neurosci. ***3***, 184–190.
31. Tian, H., Zhang, T., Jia, Y., Peng, S., and Yan, C. (2021). Zhurong: features and mission of China's first Mars rover. Innovation ***2***, 100121.
32. Zheng, Y.-C. (2020). Mars exploration in 2020. Innovation ***1***, 100036.
33. Stauffer, W.R., Lak, A., Yang, A., Borel, M., Paulsen, O., Boyden, E.S., and Schultz, W. (2016). Dopamine neuron-specific optogenetic stimulation in rhesus macaques. Cell ***166***, 1564–1571.e6.
34. Crestani, C.C., Alves, F.H., Gomes, F.V., Resstel, L.B., Correa, F.M., and Herman, J.P. (2013). Mechanisms in the bed nucleus of the stria terminalis involved in control of autonomic and neuroendocrine functions: a review. Curr. Neuropharmacol. ***11***, 141–159.
35. Piñol, R.A., Mogul, A.S., Hadley, C.K., Saha, A., Li, C., Škop, V., Province, H.S., Xiao, C., Gavrilova, O., Krashes, M.J., and Reitman, M.L. (2021). Preoptic BRS3 neurons increase body temperature and heart rate via multiple pathways. Cell Metab. ***33***, 1389–1403.e6.
36. Piñol, R.A., Zahler, S.H., Li, C., Saha, A., Tan, B.K., Škop, V., Gavrilova, O., Xiao, C., Krashes, M.J., and Reitman, M.L. (2018). Brs3 neurons in the mouse dorsomedial hypothalamus regulate body temperature, energy expenditure, and heart rate, but not food intake. Nat. Neurosci. ***21***, 1530–1540.
37. Andersen, P., and Moser, E.I. (1995). Brain temperature and hippocampal function. Hippocampus ***5***, 491–498.
38. Petersen, P.C., Vöröslakos, M., and Buzsáki, G. (2022). Brain temperature affects quantitative features of hippocampal sharp wave ripples. J. Neurophysiol. ***127***, 1417–1425.
39. Lenhardt, R. (2018). Body temperature regulation and anesthesia. Handb. Clin. Neurol. ***157***, 635–644.
40. Hunter, W.S., Holmes, K.R., and Elizondo, R.S. (1981). Thermal balance in ketamine-anesthetized rhesus monkey Macaca mulatta. Am. J. Physiol. ***241***, R301–R306.
41. Dai, J., Brooks, D.I., and Sheinberg, D.L. (2014). Optogenetic and electrical microstimulation systematically bias visuospatial choice in primates. Curr. Biol. ***24***, 63–69.
42. Dai, J., Ozden, I., Brooks, D.I., Wagner, F., May, T., Agha, N.S., Brush, B., Borton, D., Nurmikko, A.V., and Sheinberg, D.L. (2015). Modified toolbox for optogenetics in the nonhuman primate. Neurophotonics ***2***, ARTN031202.
43. Li, K., Si, L., Cui, B., Ling, X., Shen, B., and Yang, X. (2020). Altered spontaneous functional activity of the right precuneus and cuneus in patients with persistent postural-perceptual dizziness. Brain Imaging Behav. ***14***, 2176–2186.
44. Lv, J., Shi, C., Deng, Y., Lou, W., Hu, J., Shi, L., Luo, L., and Wang, D. (2016). The brain effects of laser acupuncture at thirteen ghost acupoints in healthy individuals: a resting-state functional MRI investigation. Comput. Med. Imaging Graph. ***54***, 48–54.
45. Peng, X., Lau, W.K.W., Wang, C., Ning, L., and Zhang, R. (2020). Impaired left amygdala resting state functional connectivity in subthreshold depression individuals. Sci. Rep. ***10***, 17207.

ACKNOWLEDGMENTS

We thank Dr. Robert Naumann for helpful advice. We appreciate the assistance of the SIAT MRI facility and NHP veterinaries. The work was supported by the National Natural Science Foundation of China (31871081, U20A2017, and 31871090); the Guangdong Basic and Applied Basic Research Foundation (2020B1515120072, 2009B030801037, 2020A1515010785, 2020A1515111118, and 2022A1515010134); the Shenzhen Science and Technology Program (JCYJ2018050718250547 and JCYJ20180507182458694); the Shenzhen Technological Research Center for Primate Translational Medicine, the Shenzhen Key Laboratory of Drug Addiction (ZDSYS20190902093601675); the Youth Innovation Promotion Association CAS (2017120); and the Strategic Priority Research Program of Chinese Academy of Science (XDBS01030100).

AUTHOR CONTRIBUTIONS

J.D. and H.W. designed the experiment and supervised the project; Z.Z., W.L., Y.W., F.L., and M.J. performed the experiments; Z.Z., L.S., Y.W., S.F., and J.D. analyzed the data; J.D., H.W., and Z.L. wrote the manuscript.

DECLARATION OF INTERESTS

No conflict of interest is declared.

SUPPLEMENTAL INFORMATION

It can be found online at https://doi.org/10.1016/j.xinn.2022.100358.

LEAD CONTACT WEBSITE

http://bcbdi.siat.ac.cn/index.php/member2/showMember/nid/25.shtml.